Charge transfer excitations from exact and approximate ensemble Kohn-Sham theory

Tim Gould, Leeor Kronik, and Stefano Pittalis

Citation: The Journal of Chemical Physics **148**, 174101 (2018); doi: 10.1063/1.5022832
View online: https://doi.org/10.1063/1.5022832
View Table of Contents: http://aip.scitation.org/toc/jcp/148/17
Published by the American Institute of Physics

Charge transfer excitations from exact and approximate ensemble Kohn-Sham theory

Tim Gould,[1] Leeor Kronik,[2] and Stefano Pittalis[3]
[1]*Queensland Micro- and Nanotechnology Centre, Griffith University, Nathan, Qld 4111, Australia*
[2] *Department of Materials and Interfaces, Weizmann Institute of Science, Rehovoth 76100, Israel*
[3] *CNR-Istituto Nanoscienze, Via Campi 213A, I-41125 Modena, Italy*

(Received 19 January 2018; accepted 9 April 2018; published online 1 May 2018)

By studying the lowest excitations of an exactly solvable one-dimensional soft-Coulomb molecular model, we show that components of Kohn-Sham ensembles can be used to describe charge transfer processes. Furthermore, we compute the approximate excitation energies obtained by using the exact ensemble densities in the recently formulated ensemble Hartree-exchange theory [T. Gould and S. Pittalis, Phys. Rev. Lett. **119**, 243001 (2017)]. Remarkably, our results show that triplet excitations are accurately reproduced across a dissociation curve in all cases tested, even in systems where ground state energies are poor due to strong static correlations. Singlet excitations exhibit larger deviations from exact results but are still reproduced semi-quantitatively. *Published by AIP Publishing.*
https://doi.org/10.1063/1.5022832

I. INTRODUCTION

Density functional theory[1,2] (DFT) is a widely employed approach to the many-electron problem, which has proven to be immensely useful for studying a wide range of issues in chemistry and physics. DFT is inherently a ground state theory, but its time-dependent counterpart (TDDFT)[3] is an increasingly important tool for the study of excited-state properties.

Charge transfer (CT) excitations (illustrated in Fig. 1) are physically important phenomena that are involved in key processes for energy, e.g., photosynthesis, photovoltaic energy conversion, and photocatalysis.[4–6] However, they pose a significant challenge for conventional DFT and TDDFT approximations.[7,8] The fundamental reason behind this challenge is that CT excitations involve, by definition, transitions between filled states and empty states with very little spatial overlap. As a consequence, matrix elements of the exchange-correlation kernel used in linear-response TDDFT based on Kohn-Sham (KS) theory will be vanishingly small, and excitations energies will reduce to the Kohn-Sham orbital-energy difference, unless the kernel exhibits singularity. While the exact exchange-correlation kernel does indeed exhibit such behavior,[9] standard approximate kernels do not and typically yield a drastic underestimate of the excitation energy, by as much as several eV.[10]

One useful path to overcome this problem is to capture CT transitions using constrained DFT.[11] However, this relies on prior knowledge of properties of the chemical system, which limits its range of applicability and predictive power. Optimal tuning[12] within generalized Kohn-Sham theory[13] has proven to be highly useful for prediction of both full and partial CT excitations.[8,14,15] Still, issues may arise with strongly heterogeneous systems[16] and the approach relies inherently on Fock or Fock-like operators, which can be computationally expensive. TDDFT calculations within Kohn-Sham theory, based on the exact-exchange kernel,[17–23] can, in principle, capture CT excitations, owing to a highly divergent kernel. However, this too is computationally intensive and it also lacks compatible correlation expressions. Therefore, despite much progress, there is still ongoing interest in developing additional DFT-based strategies that can capture CT excitations correctly and inexpensively.

One different low-cost route to the CT problem is afforded by the Gross, Oliveira, and Kohn (GOK)[24–26] ensemble density functional theory (EDFT),[27–33] which involves a statistical ensemble of quantum states that can be treated similarly to a ground state. EDFT can yield energy differences directly, as discussed in detail below. Indeed, excited state EDFT has seen increasing interest of late[33–40] as a potential alternative to TDDFT for excitation energies, including charge transfer excitations.[35,39] This recent resurgence of GOK EDFT mirrors a growing interest in more general forms of EDFT, which can deal, e.g., with degenerate ground states[30,41–44] and "open" systems with a non-integer number of electrons.[44–47] Furthermore, a unified EDFT could eventually offer a path to approximations that can more accurately deal with partitions or fragments of systems[48–52] as bonded fragments will naturally exchange both the charge and energy with their neighbors (that are "open"), phenomena which require an ensemble treatment.

In light of these potential advantages, it is important to understand whether exact EDFT has orbitals and densities that can acquire a direct physical meaning and are thus amenable to direct approximations, and whether approximations to EDFT, specifically exact-exchange approximations, can capture CT excitations quantitatively in a chemically illustrative case. One-dimensional molecular models with soft-Coulomb potentials provide a convenient test bed to study the first question, for both equilibrium and "stretched" chemical bonds. The recently

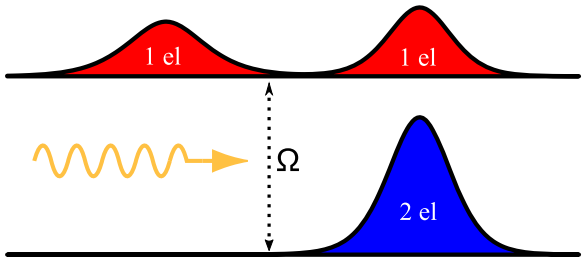

FIG. 1. An illustration of charge transfer in a dimer, from a ground state with two electrons on the right atom to an excited state with one electron on each atom. Ω is the difference in energy of the two states considered, i.e., the excitation energy.

derived ensemble Hartree-exchange (Hx) functional, $\mathcal{E}_{\rm Hx}[n]$,[33] offers theoretical tools to answer the second question, as it yields desirable multi-reference spin-states and (maximally) ghost interaction free[53] energies as an emergent property of GOK EDFT.

In this article, we will show that the answer to both questions is a qualified yes, at least for the cases considered here. This article is arranged as follows. First, we introduce GOK-EDFT and its Hartree-exchange approach. Fundamental differences with standard DFT are also spelled out. Next, we describe the model system, present the results of key tests for the lowest-energy triplet and singlet excitations, and discuss their significance. Finally, we summarize and conclude.

II. THEORY

Conventional DFT uses the electron density $n(\boldsymbol{r})$, rather than the many-electron wavefunction, as a basic variable. It thereby makes calculations much more efficient, albeit at the expense of uncontrolled approximations to the underlying physics, in the sense that the results cannot be systematically converged to the exact answer. Most DFT calculations employ the Kohn-Sham formalism,[2] which involves one-electron orbitals subject to a common potential. We start our considerations by providing a succinct overview of standard and ensemble DFT, based on the constrained minimization approach, introduced and discussed in various forms in Refs. 28–30.

A. Pure-state density functional theory

Consider a Hamiltonian $\hat{H}_v = \hat{T} + \hat{W} + \hat{v}$, where $\hat{T}$ is the kinetic energy operator, $\hat{W}$ is the electron-electron interaction operator, and $\hat{v} = \int d\boldsymbol{r} v(\boldsymbol{r})\hat{n}(\boldsymbol{r})$ is the interaction operator for electrons in an external potential $v(\boldsymbol{r})$. The ground state energy of the Hamiltonian can be found by calculating $E_0[v] = \min_\Psi \langle\Psi|\hat{H}_v|\Psi\rangle$ subject to $\langle\Psi|\Psi\rangle = 1$, with $|\Psi\rangle$ a Fermionic (antisymmetric) wavefunction, i.e., we minimize over wavefunctions.

If we instead use the Levy constrained minimization approach,[54] we can transform the process to the one where we find the ground state energy $E_0[v]$ via a minimization over the one-particle density $n(\boldsymbol{r})$, rather than wavefunctions. This involves rewriting the minimization as follows:

$$\begin{aligned} E_0[v] &= \min_\Psi \langle\Psi|\hat{H}_v|\Psi\rangle \\ &= \min_\Psi \left\{\langle\Psi|\hat{T} + \hat{W}|\Psi\rangle + \int \langle\Psi|\hat{n}(\boldsymbol{r})|\Psi\rangle v(\boldsymbol{r})d\boldsymbol{r}\right\} \\ &= \min_n \left\{ \min_{\Psi\to n}\langle\Psi|\hat{T} + \hat{W}|\Psi\rangle + \int n(\boldsymbol{r})v(\boldsymbol{r})d\boldsymbol{r}\right\} \\ &\equiv \min_n \left\{F[n] + \int n(\boldsymbol{r})v(\boldsymbol{r})\right\}. \end{aligned} \tag{1}$$

Here, the intermediate steps define a functional of the particle density $F[n]$ that depends only on the form of the kinetic and interaction energy operators and does not depend on the external potential. The constraint $\Psi \to n$ in the penultimate expression means the minimization is taken only over normalized Fermionic wavefunctions obeying $\langle\Psi|\hat{n}|\Psi\rangle = n(\boldsymbol{r})$, i.e., constrained to the desired (N-representable) density $n(\boldsymbol{r})$.

The ground state density can be found also by solving the ground state of the Kohn-Sham system. Kohn-Sham DFT can be viewed from the perspective of the adiabatic connection,[55] in which electron-electron interactions are scaled by λ. This generalizes the universal density functional $F[n]$ to

$$F^\lambda[n] = \min_{\Psi\to n}\langle\Psi|\hat{T} + \lambda\hat{W}|\Psi\rangle \tag{2}$$

(again with $|\Psi\rangle$ Fermionic and normalized). The constrained minimization in (2) can be solved, for "typical" v-representable densities $n(\boldsymbol{r})$, by finding the representative potential $v^\lambda[n](\boldsymbol{r})$ for which the ground state $|\Psi^{n,\lambda}\rangle$ of $\hat{H}^\lambda = \hat{T} + \lambda\hat{W} + \int v^\lambda[n]\hat{n}d\boldsymbol{r}$ obeys $n = \langle\Psi^{n,\lambda}|\hat{n}|\Psi^{n,\lambda}\rangle$ (this is the definition of a v-representable pure state density n). In such cases, v^λ serves as a Lagrange multiplier in the calculation of F^λ, and thus $F^\lambda[n] = \langle\Psi^{n,\lambda}|\hat{T} + \lambda\hat{W}|\Psi^{n,\lambda}\rangle$. At full-interaction strength $\lambda = 1$, the corresponding potential $v^1 = v$ is simply the external potential of the many-electron system. With no interactions, $v_s \equiv v^0$ is known as the Kohn-Sham (KS) potential and, due to the absence of two-body interactions, with the exception of degenerate ground states, $|\Psi^{n,0}\rangle \equiv |\Phi_s\rangle$ is unambiguously a *single* Slater-determinant wavefunction.

From these basic definitions, we can further define two other key functionals, the non-interacting kinetic energy and the Hartree-exchange (Hx) functionals,

$$T_s[n] \equiv F^0[n] = \langle\Phi_s|\hat{T}|\Phi_s\rangle, \tag{3}$$

$$E_{\rm Hx}[n] \equiv \langle\Phi_s|\hat{W}|\Phi_s\rangle. \tag{4}$$

Both functionals can be defined in terms of a set of numerically convenient one-particle orbitals $\{\phi_i\}$, from which the Slater determinant wavefunction, $|\Phi_s\rangle$ for $\lambda = 0$, is constructed. These orbitals are defined to be unoccupied, occupied singly or in spin-pairs, giving occupation factors $f_i \in \{0, 1, 2\}$. Thus, e.g., we can write $T_s = \sum_i f_i\langle\phi_i|\hat{t}|\phi_i\rangle$ for the KS kinetic energy and $n = \langle\Phi_s|\hat{n}|\Phi_s\rangle = \sum_i f_i|\phi_i|^2 \equiv \langle\Psi^{n,1}|\hat{n}|\Psi^{n,1}\rangle$ for the density. The orbitals obey the Kohn-Sham equation

$$\{\hat{t} + v_s[n](\boldsymbol{r})\}\phi_i[n](\boldsymbol{r}) = \epsilon_i[n]\phi_i[n](\boldsymbol{r}). \tag{5}$$

Here $\hat{t} = -\frac{1}{2}\nabla^2$ and $v_s[n] \equiv v^0[n]$ is the single-particle multiplicative Kohn-Sham potential, which is the fictitious effective potential experienced by the orbitals.

The Kohn-Sham formulation of DFT therefore transforms a difficult many-electron problem into a simpler non-interacting one. The remaining complexity is bundled into a

correlation term $E_c[n] = F^1[n] - T_s[n] - E_{Hx}[n]$, which is also a functional of the density n. E_c is highly non-trivial in general, but can be usefully approximated—typically, but not always, in combination with the exchange part $E_x[n]$ of $E_{Hx}[n]$ (as $E_{xc}[n]$) to allow for error cancellation. Many useful approximations for E_{xc} exist that allow DFT to be used cheaply in a predictive fashion (see, e.g., Refs. 56–60). When the correlation component is set to zero but the other quantities are evaluated exactly, one ends up with the "exact exchange" approximation.

B. Ensemble density functional theory

DFT was originally conceived as a theory of pure-states and in its original form provides direct access only to properties of the ground state, notably its electron density and energy. DFT was later generalized to the case of ensembles,[27,28] which can be broadly categorized into three forms: First, there are ensemble of states with different numbers of electrons in each state;[29] second, ensembles may be required to deal with degenerate ground states;[61] and finally, Gross, Oliveira, and Kohn (GOK) ensembles[24–26] extend density functional theory to statistical ensembles of eigenstates.

Specifically, the GOK ensemble DFT (EDFT) replaces a single ground state wavefunction by a density matrix,

$$\hat{\Gamma}_{\mathcal{W}} = \sum_{\kappa} w_\kappa |\Psi_\kappa\rangle\langle\Psi_\kappa|, \qquad \sum_{\kappa} w_\kappa = 1, \tag{6}$$

where $\langle\Psi_\kappa|\Psi_{\kappa'}\rangle = \delta_{\kappa\kappa'}$, and where the set of positive weights $\mathcal{W} \equiv \{w_\kappa\}$ obeys certain constraints discussed below. Following a similar sequence of steps to Eq. (1), the ensemble energy can be calculated through

$$\begin{aligned}\mathcal{E}[v;\mathcal{W}] &= \min_n \left\{\mathcal{F}^1[n;\mathcal{W}] + \int n(\boldsymbol{r})v(\boldsymbol{r})d\boldsymbol{r}\right\} \\ &\equiv \sum_{\kappa} w_\kappa E_\kappa[v],\end{aligned} \tag{7}$$

where the minimization is performed over the *statistically averaged* density $n = \sum_\kappa w_\kappa\langle\Psi_\kappa|\hat{n}|\Psi_\kappa\rangle$, and where $E_\kappa[v]$ are the low lying eigenvalues (energies) of the many-electron Hamiltonian $\hat{H}_v$.

One can then invoke the ensemble version of $F^\lambda[n]$,

$$\mathcal{F}^\lambda[n;\mathcal{W}] = \min_{\hat{\Gamma}_{\mathcal{W}}\to n} \mathrm{Tr}[\hat{\Gamma}_{\mathcal{W}}(\hat{T} + \lambda\hat{W})], \tag{8}$$

which is subject, as above, to constrained minimization such that $\mathrm{Tr}[\Gamma_{\mathcal{W}}\hat{n}] \equiv \sum_\kappa w_\kappa\langle\Psi_\kappa|\hat{n}|\Psi_\kappa\rangle = n(\boldsymbol{r})$ and defined for given "well-behaved" sets of fixed weights $\mathcal{W} = \{w_\kappa\}$. Thus, $\mathcal{E}$ now equals a statistical average of the lowest lying energy eigenvalues $E_\kappa[v]$ of $\hat{H}_v = \hat{T} + \hat{W} + \int \hat{n}(\boldsymbol{r})v(\boldsymbol{r})d\boldsymbol{r}$ for weights $\mathcal{W} = \{w_\kappa\}$ obeying $\sum w_\kappa = 1, 0 \le w_\kappa \le 1, w_\kappa \ge w_{\kappa'}$ for $E_\kappa \le E_{\kappa'}$ and other conditions discussed in detail in the original GOK articles[24–26] and in more recent work.[33]

As above for the pure state, we can implicitly define a density matrix $\hat{\Gamma}^{n,\lambda}_{\mathcal{W}} \equiv \sum_\kappa w_\kappa|\Psi^{n,\lambda}{}_\kappa\rangle\langle\Psi^{n,\lambda}{}_\kappa|$ using $\mathrm{Tr}[\hat{\Gamma}^{n,\lambda}_{\mathcal{W}}(\hat{T} + \lambda\hat{W})] = \mathcal{F}^\lambda[n;\mathcal{W}]$, i.e., $\hat{\Gamma}^{n,\lambda}_{\mathcal{W}}$ is any density matrix that minimizes the trace which, in many cases, will not be unique. Similarly, we can extend the idea of an *ensemble v* representable density[32] to the one for which the eigenstates $|\Psi^{n,\lambda}{}_\kappa\rangle$ in $\hat{\Gamma}^{n,\lambda}_\kappa$ obey $[\hat{T} + \lambda\hat{W} + \hat{v}^\lambda - E^{n,\lambda}_\kappa]|\Psi^{n,\lambda}{}_\kappa\rangle = 0$ with $v^1 = v$ and, analogously to the pure ground state case, $v_s[n,\mathcal{W}] \equiv v^0$. The wavefunctions $|\Phi_{s,\kappa}\rangle \equiv |\Psi^{n,0}_\kappa\rangle$ can then be written as a set of orthogonal Slater determinants. Pure-state DFT, per Eq. (1), is the special case $w_0 = 1$ and $w_{\kappa>0} = 0$.

Thus, DFT can be generalized to include an ensemble like that of (6), formed using a fixed set of ensemble weights $\mathcal{W} = \{w_\kappa\}$, which, as before, can be written in terms of a set of occupied KS orbitals obeying

$$\{\hat{t} + v_s[n;\mathcal{W}]\}\phi_i[n;\mathcal{W}] = \epsilon_i[n;\mathcal{W}]\phi_i[n;\mathcal{W}], \tag{9}$$

where

$$v_s[n;\mathcal{W}](\boldsymbol{r}) \equiv v(\boldsymbol{r}) + v_{Hxc}[n;\mathcal{W}](\boldsymbol{r}) \tag{10}$$

is the ensemble Kohn-Sham potential. Here the one-body system depends on $n = \sum_i f_i|\phi_i|^2$, as above. A key difference, however, is that we must consider also the set of weights $\mathcal{W}$—*each unique set of weights defines a unique functional in a rigorous fashion*. This generalization away from a pure ground state allows the Kohn-Sham occupation factors $f_i[n,\mathcal{W}] \in [0,2]$ to take on non-integer values in a rigorous fashion. Related discussion on the topic of non-integer ensembles can be found in Ref. 62.

One can now ensemble-generalize other functionals. The non-interacting kinetic energy functional, $\mathcal{T}_s[n;\mathcal{W}]$, is readily given by

$$\mathcal{T}_s[n;\mathcal{W}] \equiv \mathcal{F}^0[n;\mathcal{W}] \equiv \sum_i f_i\langle\phi_i|\hat{t}|\phi_i\rangle\,. \tag{11}$$

Given the density $n(\boldsymbol{r})$ and set of fixed ensemble weights $\mathcal{W} = \{w_\kappa\}$, there also exists a unique Hartree-exchange energy functional, given by[33]

$$\begin{aligned}\mathcal{E}_{Hx}[n;\mathcal{W}] &= \lim_{\lambda\to 0^+} \frac{\mathcal{F}^\lambda[n;\mathcal{W}] - \mathcal{T}_s[n;\mathcal{W}]}{\lambda} \\ &\equiv \sum_\kappa w_\kappa \Lambda_{Hx,\kappa}[n;\mathcal{W}].\end{aligned} \tag{12}$$

Thus, the Hartree-exchange functional, $\mathcal{E}_{Hx}[n;\mathcal{W}]$, can be defined even though $\hat{\Gamma}^{n,\lambda=0}_{\mathcal{W}}$ is not necessarily unique. Equation (12) involves a set of unique Hx energy functionals, $\Lambda_{Hx,\kappa}[n]$, one for each weight w_κ, which are "block eigenvalues" of an interaction matrix $\mathbb{W} = W_{\kappa\kappa'} = \langle\Phi_{s,\kappa}|\hat{W}|\Phi_{s,\kappa'}\rangle$, involving only the set of Kohn-Sham non-interacting Slater determinant states $|\Phi_{s,\kappa}\rangle$ included in the non-interacting ensemble. This means that $\mathcal{E}_{Hx}$ is a functional of the (partially) occupied orbitals only. It can be shown[33] that the energy functionals $\Lambda_{Hx,\kappa}$ naturally allow the overall functional to directly adapt to fundamental spin symmetries without any external inputs or assumptions, even when multi-reference physics is required. The above definition reduces to the combined Hartree-exchange proposed earlier by Nagy[42] and to the symmetry-eigenstate Hartree-exchange (SEHX) expression[38] in certain special cases, including the one presented here. The work by Filatov[35,36] uses similar principles to those espoused in Ref. 33 to show how EDFT can help with approximating strong correlations, for both ground and excited states.

In the "ensemble exact exchange" (EEXX) approximation, $\mathcal{T}_s[n;\mathcal{W}]$ and $\mathcal{E}_{Hx}[n;\mathcal{W}]$ are evaluated exactly but correlation (via ensemble-generalized $\mathcal{E}_c[n;\mathcal{W}] = \mathcal{F}^1[n;\mathcal{W}] - \mathcal{T}_s[n;\mathcal{W}] - \mathcal{E}_{Hx}[n;\mathcal{W}]$) is neglected. In recent years, significant progress in understanding and utilizing the EEXX

approximation has been made. Yang, Pribram-Jones, and coworkers used symmetry arguments to define a symmetry-eigenstate Hartree-exchange (SEHX) approximation, which they used successfully to show that EEXX calculations can yield good results in small atoms and various model systems.[38–40] Recently, Gould and Pittalis have noted, by resolving the issue of non-uniqueness in the definition of the "Hx" term, that SEHX may be regarded as a useful special case of an EEXX formalism derived directly from the interaction-dependent ensemble universal functional.[33]

Importantly, EEXX can be calculated in two ways: it can be obtained as a functional of the exact density, using the exact orbitals; or, more commonly, it is performed using orbitals obtained self-consistently through an optimized effective potential approach.[63,64] Here, we pursue the former approach because we are interested in the ultimate accuracy afforded by the EEXX functional. Therefore, we avoid density-driven errors,[65] i.e., errors in the EEXX energies that do not arise from the EEXX functional itself, but rather from its self-consistent application without a compatible correlation expression. The effect of self-consistency will be taken up elsewhere. Details of $\mathcal{E}_{\rm Hx}$ that are relevant to the cases considered in the remainder of this manuscript are discussed in greater detail in Appendix A.

C. A numerically solvable model of CT excitations

We choose a simple model diatom system possessing two electrons in a one-dimensional and (controllably) asymmetric diatomic molecule. We define

$$\hat{H} = \hat{T} + \hat{W} + \hat{v}, \tag{13}$$

where the kinetic energy operator is $\hat{T} = \hat{t} + \hat{t}'$ with $\hat{t} = -\frac{1}{2}\frac{d^2}{dx^2}$, the external potential operator is $\hat{v} = \int dx \hat{n}(x) v(x)$, and the interaction operator is $\hat{W} = \int \frac{dx dx'}{2} \hat{n}_2(x,x') U(x-x')$, where $\hat{n}_2(x,x') = \hat{n}(x)\hat{n}(x') - \delta(x-x')\hat{n}(x)$. Here we employ a soft-Coulomb potential, $U(z) = (\frac{1}{4} + z^2)^{-\frac{1}{2}}$, for Coulomb interactions. For the external potential, we use

$$v(x) = -U(x + R/2) - \left[U(x - R/2) + \mu_S e^{-(x-R/2)^2}\right]. \tag{14}$$

Here R is the bond length between the left atom lying at $-R/2$ and the right atom lying at $+R/2$. The term μ_S changes the well depth on the right atom, with larger μ_S making the well deeper. By adopting the soft-Coulomb interaction in all terms, including the nuclear potential, we are able to test the appropriateness of the approach across the entire dissociation curve, including energetics resulting from attraction/cancellation of nuclear charges by electronic densities.

By varying μ_S, we are able to change the form of the ground state in the dissociation limit, $R \to \infty$. For $\mu_S = 0$, symmetry ensures that both the left and right atoms have one electron each. By contrast, for $\mu_S = 2.0$, the dissociation limit leads to two electrons on the right atom, and none on the left, with the change in asymptotic behavior occurring for $\mu_S \approx 1.4$. Numerically, we find that for $0 \le \mu_S \le 2$ the triplet state always involves one electron on each of the two nuclei, meaning that for sufficiently large R and μ_S, the lowest energy excitation involves transferring charge from the right atom to the left atom, as in Fig. 1. Thus we have a numerically solvable model which contains the key physics we wish to study, namely, charge transfer excitations.[66]

We denote the ground state as $|\text{gs}\rangle \equiv |\Psi_0^{n,1}\rangle$. For reasons of pedagogical simplicity, here we focus on the lowest energy singlet-triplet transition and denote the lowest triplet excited state, $|\text{ts}\rangle \equiv |\Psi_1^{n,1}\rangle$ (singlet excitations are discussed in Sec. III B). If we set $w_0 = 1 - p$ and $w_1 = p$, we can define an ensemble $\hat{\Gamma}^{n,1} = (1-p)|\Psi_0^{n,1}\rangle\langle\Psi_0^{n,1}| + p|\Psi_1^{n,1}\rangle\langle\Psi_1^{n,1}| = (1-p)|\text{gs}\rangle\langle\text{gs}| + p|\text{ts}\rangle\langle\text{ts}|$ that is equivalent to having a probability p of being in the three-fold degenerate lowest excited state and a probability $(1-p)$ of being in the ground state. This degeneracy is a direct consequence of the exact formalism adopted throughout this work, which we discuss in greater detail later. We can then rewrite Eq. (7) as

$$\begin{aligned}\mathcal{E}[v,p] &= \mathcal{F}^1[n^{(p)},p] + \int n^{(p)}(x)v(x)dx, \\ &= w_{\rm gs}E_{\rm gs} + w_{\rm ts}E_{\rm ts} = E_{\rm gs} + p[E_{\rm ts} - E_{\rm gs}],\end{aligned} \tag{15}$$

where $n^{(p)} = n_{\rm gs} + p[n_{\rm ts} - n_{\rm gs}]$ is the density of the ensemble system [parametrized using p, as indicated by the superscript (p)] with external potential v. Thus, we obtain an energy that depends linearly on the excitation energy $E_{\rm ts} - E_{\rm gs}$, which allows us to use Eq. (7) to calculate energy differences by varying p. Here and henceforth, we restrict the set of weights $\mathcal{W}$ to provide such an admixture of the ground- and excited states only, i.e., we set $w_0 = 1 - p$, $w_1 = p$, and $w_{\kappa>2} = 0$ as above. We can therefore adopt a short-hand notation, $\mathcal{E}^{(p)} \equiv \mathcal{E}[n = n^{(p)}, \mathcal{W} = \{1-p, p\}]$.

We can determine the exact eigenstates of our model Hamiltonian (13) using simple numerics implemented in Python with NumPy and SciPy. This lets us calculate properties, such as energies, energy differences, and densities for the true ensemble $\hat{\Gamma}^{n,1}$. From the exact results, we can then use density inversion techniques for EDFT[67] to obtain the non-interacting KS reference system. This involves finding a multiplicative potential, $v_s^{(p)}$, that yields single-particle orbital solutions of

$$\{\hat{t} + v_s^{(p)}(\boldsymbol{r})\}\phi_i^{(p)}(\boldsymbol{r}) = \epsilon_i^{(p)}\phi_i^{(p)}(\boldsymbol{r}) \tag{16}$$

such that they correctly reproduce the target density, i.e.,

$$\begin{aligned}n^{(p)} &= (1-p)n_{\rm gs} + pn_{\rm ts} = (1-p)n_{s,\rm gs}^{(p)} + pn_{t,\rm ts}^{(p)} \\ &= (2-p)|\phi_0^{(p)}|^2 + p|\phi_1^{(p)}|^2,\end{aligned} \tag{17}$$

where the last line uses the relations $n_{s,\rm gs}(\boldsymbol{r}) = 2|\phi_0(\boldsymbol{r})|^2$ and $n_{s,\rm ts}(\boldsymbol{r}) = |\phi_0(\boldsymbol{r})|^2 + |\phi_1(\boldsymbol{r})|^2$, which connect between the densities of the Kohn-Sham ensemble members and the Kohn-Sham orbitals. When (16) and (17) are simultaneously satisfied, $v_s^{(p)} \equiv v + v_{\rm Hxc}^{(p)}$ is the exact Kohn-Sham potential and, thus, $v_{\rm Hxc}^{(p)}$ is the exact Hartree-exchange-correlation potential.

Importantly, the exact-ensemble solutions found here do not break spin-symmetry, or the mirror symmetry of H_2 for $\mu_S = 0$. This gives the KS system the same multiplet structure as the interacting system—a highly desirable feature,[68] especially when identifying excitations in complex situations. The exact KS orbitals allow us to calculate all the reference data for the analyses reported in Sec. III and compare to approximate

data. For our tests, we make the Kohn-Sham ensemble exact exchange (EEXX) approximation,

$$\mathcal{F}[n,\mathcal{W}] \approx \mathcal{T}_s[n,\mathcal{W}] + \mathcal{E}_{\rm Hx}[n,\mathcal{W}], \tag{18}$$

as an extension of its ground state counterpart, i.e., our only approximation is to set $\mathcal{E}_{\rm c}[n,\mathcal{W}] \equiv 0$. Thus, for arbitrary p and exact orbitals $\phi_i^{(p)}$, we have

$$\mathcal{E}^{(p)}_{\rm EEXX} = \mathcal{T}_s^{(p)} + \mathcal{E}^{(p)}_{\rm Hx} + \int n^{(p)} v\,dx \tag{19}$$

$$\equiv (1-p)\{T^{(p)}_{s,\rm gs} + \Lambda^{(p)}_{\rm Hx,gs}\} + p\{T^{(p)}_{s,\rm ts} + \Lambda^{(p)}_{\rm Hx,ts}\} + \int n^{(p)} v\,dx. \tag{20}$$

The kinetic and interaction energy terms have implicit (via the orbitals) and explicit p dependencies. The kinetic energy terms for the states are

$$T^{(p)}_{s,\rm gs} = 2t_0^{(p)}, \qquad T^{(p)}_{s,\rm ts} = t_0^{(p)} + t_1^{(p)},$$

where $t_i = \int \phi_i(x)\hat{t}\phi_i(x)dx$ and all orbitals ϕ_i are real. The interaction energy terms,

$$\Lambda^{(p)}_{\rm Hx,gs} = \int \frac{dxdx'}{2} U(x-x') 2\phi_0^{(p)}(x)^2 \phi_0^{(p)}(x')^2, \tag{21}$$

$$\Lambda^{(p)}_{\rm Hx,ts} = \int \frac{dxdx'}{2} U(x-x') \times [\phi_0^{(p)}(x)\phi_1^{(p)}(x') - \phi_1^{(p)}(x)\phi_0^{(p)}(x')]^2, \tag{22}$$

are defined according to the underlying symmetries of the singlet-, ground-, and triplet excited states—which follows directly from the definition of $\mathcal{E}_{\rm Hx}$[33] (see Appendix A for details).

III. RESULTS

Having established the theory and model systems, we now report the results of several tests that examine the successes and limitations of the proposed EDFT approach.

A. Triplet states

First, we establish that exact EDFT does indeed capture the nature of charge transfer excitations. To this end, we now consider the density components that comprise the statistical ensemble, in order to examine the ability of the approach to "move" charge during excitations (as illustrated in Fig. 1, where one electron is moved from the right atom to the left one under excitation).

We determine charge densities for the ground and triplet states in two different ways. First, we denote $n_{\rm gs} = \langle {\rm gs}|\hat{n}|{\rm gs}\rangle$ and $n_{\rm ts} = \langle {\rm ts}|\hat{n}|{\rm ts}\rangle$ to be the true electron densities of the ground state and triplet wavefunctions, respectively. Next, $n^{(p)}_{s,\rm gs}(x) = 2\phi_0^{(p)}(x)^2$ and $n^{(p)}_{s,\rm ts}(x) = \phi_0^{(p)}(x)^2 + \phi_1^{(p)}(x)^2$ are the densities of the corresponding Kohn-Sham states $|\Phi_{s,\rm gs/ts}\rangle$, obtained by minimizing $\mathcal{T}_s = \mathcal{F}^0$ subject to the constraints. Note that generally $n_{\rm gs} \neq n^{(p)}_{s,\rm gs}$ (except for $p=0$) and $n_{\rm ts} \neq n^{(p)}_{s,\rm ts}$, i.e., the KS ground-state and triplet state densities do not need to be the same as the exact ones even in exact EDFT. Only the statistical average of the KS density must equal that of the density of the interacting system, i.e., $n^{(p)} = (1-p)n_{\rm gs} + pn_{\rm ts} = (1-p)n^{(p)}_{s,\rm gs} + pn^{(p)}_{s,\rm ts} = n_s^{(p)}$ [cf. Eq. (17) and see Appendix B for further discussion].

Figure 2 shows the interacting-system (solid lines) and exact Kohn-Sham (dashed lines) densities, as obtained from the above-described inversion process, for the case of $R = 4$ and $\mu_S = 2$ with $p = 0$, $p = 0.2$, and $p = 0.5$. For all p, the ground-state and triplet densities of the real and KS states, while indeed not equal, are clearly similar, demonstrating a genuine ability of the EDFT to transfer charge spatially. This is a non-trivial result as the individual KS densities are only constrained by their ensemble average. Thus, e.g., in the case $p = 0.5$, the KS system could have had 1.5 electrons on the right atom and 0.5 electrons on the left atom in both the ground and triplet states, as in the total density. The fact that the individual KS densities resemble their exact counterparts, with 2 electrons on the right atom for the ground state and 1 electron on each atom for the triplet state, is therefore a success of KS EDFT. Filatov *et al.* have similarly shown that approximations to EDFT can describe transfer of charge in excitations of the 4-(*N*,NDimethyl-amino)benzonitrile (DMABN)

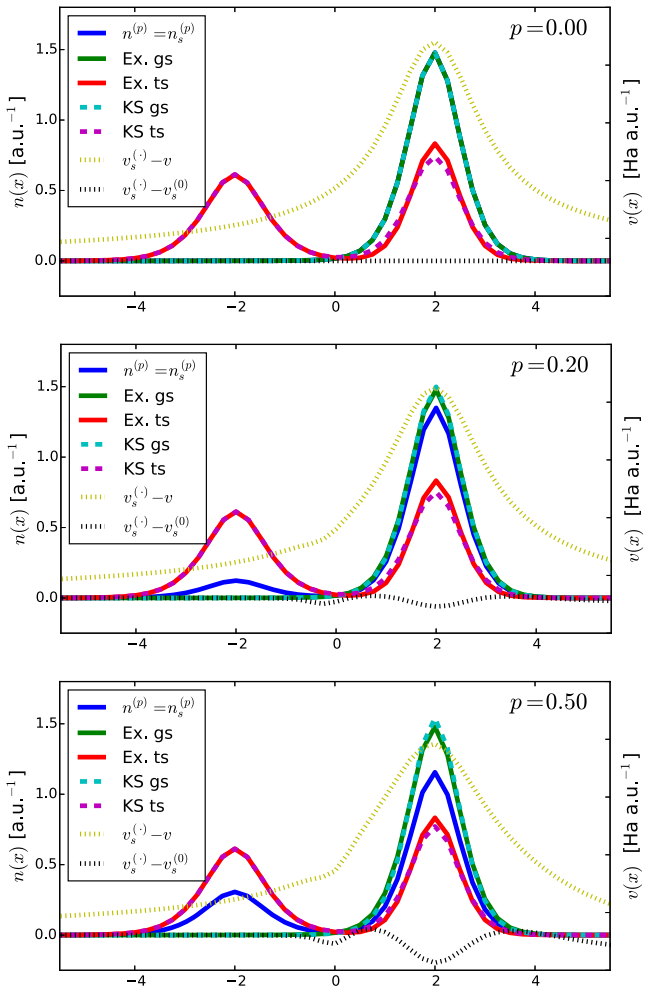

FIG. 2. Exact ($n_{\rm gs/ts}$, solid lines) and Kohn-Sham ($n^{(p)}_{s,\rm gs/ts}$, dashed lines) densities of the ground- and first excited states with $R = 4$ and $\mu_S = 2.0$, calculated from the interacting and non-interacting wavefunctions, respectively. Top: $p = 0$, middle: $p = 0.2$, bottom: $p = 0.5$. In all cases, the KS states are found to be good representations of the exact densities despite not being under any "formal" obligation to be so. Also shown (in dotted lines) are the Hxc potential, $v^{(p)}_{\rm Hxc} = v_s^{(p)} - v$, and the ensemble potential difference, $v_s^{(p)} - v_s^{(0)}$.

chromophore, albeit without direct comparison to the densities associated with the exact transitions.[35]

The plots in Fig. 2 also include (as dotted lines) the exact Hartree-exchange-correlation potential $v_{\rm Hxc}^{(p)} = v_s^{(p)} - v$, as well as the difference between the KS potential obtained at finite p with that obtained for the pure ground state, i.e., $v_s^{(p)} - v_s^{(0)}$. Importantly, it is well known that in open electron-number ensemble systems, the addition of a small amount of additional charge can lead to difficult-to-approximate step features.[29,67,69,70] The exact potentials plotted in Fig. 2 exhibit no such features. This highlights a potential advantage of EDFT over alternative approaches, in that the ensemble correction to the KS system may lend itself to future approximations involving semi-local functionals that cannot produce step-like features.

Having established the validity and potential usefulness of the EDFT approach, we turn to examining energy differences in charge transfer states. We have already established that $\mathcal{E}^{(p)} = E_{\rm gs} + p(E_{\rm ts} - E_{\rm gs})$, where $E_{\rm gs}$ and $E_{\rm ts}$ are defined for a given v that is determined by R and μ_S, with the pure ground state, $E_{\rm gs} = \mathcal{E}^{(0)}$, obtained for $p = 0$. For the exact functional, the energy is then a straight line in p, without any implicit dependence on p, yielding

$$\Omega \equiv E_{\rm ts} - E_{\rm gs} = \frac{\mathcal{E}^{(p)} - \mathcal{E}^{(0)}}{p} = \frac{\partial \mathcal{E}^{(p)}}{\partial p} \tag{23}$$

for the exact excitation energy (optical gap) from the ground to triplet state. We can compare these exact results to approximate ones obtained using the exact-exchange expression [Eq. (20)], where the correlation energy is neglected. This means that the approximate expressions,

$$\Omega_{\rm EEXX}^{(p)} \equiv \frac{\mathcal{E}_{\rm EEXX}^{(p)} - \mathcal{E}_{\rm EEXX}^{(0)}}{p} \tag{24}$$

or

$$\Omega'^{(p)}_{\rm EEXX} \equiv \frac{\partial \mathcal{E}_{\rm EEXX}^{(p)}}{\partial p}, \tag{25}$$

are neither necessarily the same nor necessarily independent of p due to implicit dependencies on the orbitals. Non-linearities in this context were first discussed by Gross, Oliveira, and Kohn[25] and were previously analysed for GOK and other ensembles in various studies.[39,44,45,71]

The results of the exact calculations for Ω, compared with approximate ones obtained using both EEXX excitation expressions given above, at different values of p, are given in Fig. 3. We use $\mu_S = 2$, which corresponds to a charge transfer molecule, and study both $R = 0.5$ and $R = 4$. Importantly, here and below, the approximate results are not obtained self-consistently, but rather from the approximate energy expression based on the exact densities. This allows us to focus on errors due to the approximate functional and eliminate errors due to an approximate density.[65] Figure 3 shows that the approximate expressions yield results that are within a few tenths of an eV of each other and in generally similar agreement with exact results, with the non-derivative expression (24) yielding a curve that is somewhat flatter and in better agreement with the exact value. This is quite satisfactory, given that no correlation energy is included.

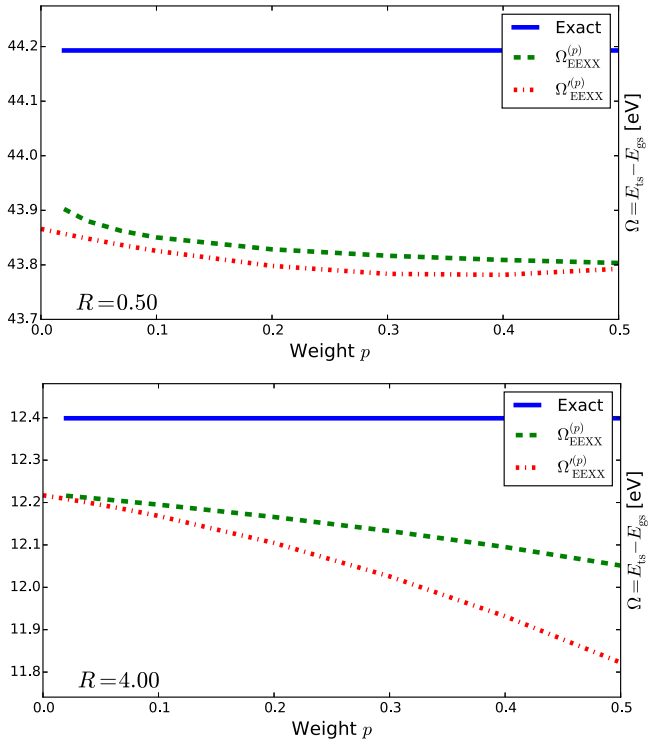

FIG. 3. Exact energy gap (as obtained in both the many-electron and the exact Kohn-Sham system), compared with that obtained in the EEXX approximation calculated in two different ways, based on $\Omega_{\rm EEXX}$ and $\Omega'_{\rm EEXX}$ [Eqs. (24) and (25)], with $R = 0.5$ (top) and $R = 4$ (bottom) and $\mu_S = 2.0$, which defines a clear charge transfer excitation. The difference between $\Omega_{\rm EEXX}$ and $\Omega'_{\rm EEXX}$ for $W \to 0$ for $R = 0.5$ is due to numerical errors.

Finally, we consider the ability of EEXX to reproduce dissociation curves for either the ground state or the triplet state, defined by $\Delta E_{\rm gs/ts}(R) = E_{\rm gs/ts}(R) - E_{\rm gs}(R \to \infty) + U(R)$, where the penultimate term is the ground-state energy at the full dissociation limit and the final term is the inter-nuclear repulsion energy. A comparison between EEXX and exact EDFT is given in Fig. 4, where results are shown for two strongly correlated dimers ($\mu_S = 0$ and 1.2) and two charge-transfer dimers ($\mu_S = 1.6$ and 2). The triplet-state EEXX results were obtained via the relation

$$E_{\rm EEXX,ts}(R) \equiv E_{\rm EEXX,gs}(R) + \Omega_{\rm EEXX}^{(0.5)}(R), \tag{26}$$

where $\Omega_{\rm EEXX}^{(0.5)}(R) = 2[\mathcal{E}_{\rm EEXX}^{(0.5)}(R) - \mathcal{E}_{\rm EEXX}^{(0)}(R)]$, i.e., the excitation energy is evaluated at the maximal mixing point, $p = 0.5$, using a difference formula.

Clearly, for the charge-transfer dimers, ground-state dissociation curves are well reproduced by EEXX. However, for the strongly correlated dimers, the ground-state dissociation curves are very poorly reproduced, to the point that the ground state energies become *greater* than the excited state in the dissociation limit, which means that the predicted Kohn-Sham excitation energy is *negative*, at the Hx level. The failure of a zero-correlation expression in the strong correlation limit is not at all surprising in itself. What may seem counter-intuitive, however, is the negative excitation energy. This is because DFT, even in GOK ensemble form, is a theory of lowest energy states and thus one expects that other states

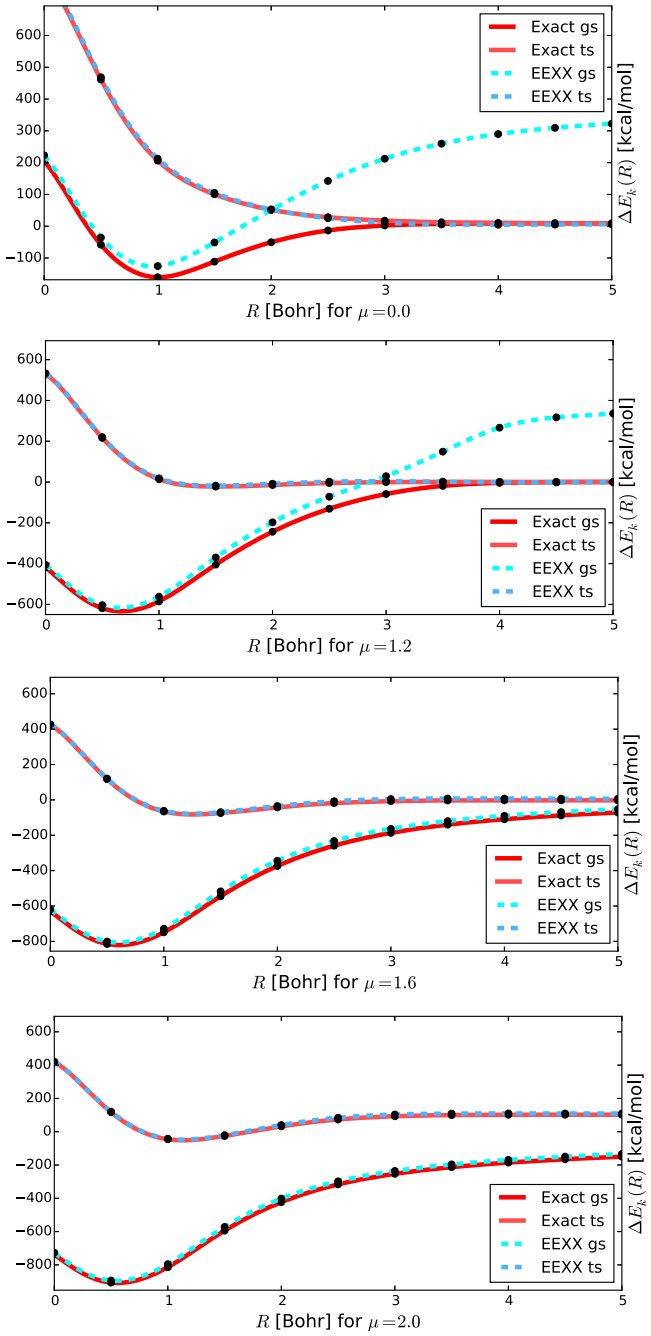

FIG. 4. Exact and Hartree-exchange energy dissociation curves for the ground state and triplet state for $\mu_S = 0$ (top), 1.2 (second), 1.6 (third), and 2 (bottom). EEXX energies are obtained using Eq. (26). Remarkably, in all cases, Hartree-exchange energies are excellent approximations to the triplet energy, even when strong static correlation results in very poor ground state energies that can even be greater in energy than the excited state.

should be energy-ordered accordingly under any DFT approximation. Nevertheless, this result is perfectly in line with the theory because the universal functional $\mathcal{F}[n, \mathcal{W}]$ is defined for a *given choice* of $\mathcal{W}$ and n. Thus, when we choose $p = 0$ and $p = 0.5$, we are using *different density functionals* and there is no issue with ordering when comparing energies as we do here.

Remarkably, triplet-energy dissociation curves for the charge-transfer dimers are well reproduced at all R and for *all* dimers, including the most correlated H_2 molecule ($\mu_S = 0$), despite a ground state that is a very poor approximation for the strongly correlated true ground state.[72] Indeed, a higher-quality triplet state, compared to the ground state, was reported previously using hybrid functional theory in the context of triplet instabilities.[73]

B. Singlet states

As mentioned in our introduction of the model system, we have focused on the lowest energy singlet-triplet transition for reasons of pedagogical simplicity. However, this poses significant limitations. First, the singlet-triplet transition is "optically dark" and therefore of less practical interest; second, it is actually amenable to analysis using conventional ground state DFT, if appropriate spin-symmetry restrictions are imposed. Therefore, in this section, we discuss a more general ensemble that includes contributions from the lowest-lying excited singlet state and use it to study the physically important, and more difficult to reproduce, singlet CT excitation.

Consider a GOK ensemble with a mixture of $p \leq \frac{1}{2}$ triplet and singlet excited states, of which a fraction, $\beta \leq \frac{1}{4}$, is in the singlet state. (The upper bounds come from the general condition on GOK ensemble weights that $w_\kappa \geq w_{\kappa'}$ when $E_\kappa \leq E_{\kappa'}$.) Therefore, we have

$$\hat{\Gamma} = (1-p)|\mathrm{gs}\rangle\langle\mathrm{gs}| + p(1-\beta)|\mathrm{ts}\rangle\langle\mathrm{ts}| + p\beta|\mathrm{ss}\rangle\langle\mathrm{ss}|, \quad (27)$$

where $|ss\rangle$ is the first excited singlet state. This yields

$$\mathcal{E}^{(p;\beta)} = E_{\mathrm{gs}} + p[(E_{\mathrm{ts}} - E_{\mathrm{gs}}) + \beta(E_{\mathrm{ss}} - E_{\mathrm{ts}})] \quad (28)$$

(note $\mathcal{E}^{(p;0)} \equiv \mathcal{E}^{(p)}$) and

$$\begin{aligned} n^{(p;\beta)} &= (1-p)n_{\mathrm{gs}} + p[(1-\beta)n_{\mathrm{ts}} + \beta n_{\mathrm{ss}}] \\ &= (1-p)n_{s,\mathrm{gs}}^{(p;\beta)} + pn_{s,\mathrm{ts}}^{(p;\beta)} \\ &= (2-p)|\phi_0^{(p;\beta)}|^2 + p|\phi_1^{(p;\beta)}|^2 , \end{aligned} \quad (29)$$

for the energy and density, respectively. Here we used $n_{s,\mathrm{ts}} = n_{s,\mathrm{ss}} = |\phi_0|^2 + |\phi_1|^2$, which follows directly from the KS ensemble minimization. The kinetic energy $\mathcal{T}_s^{(p;\beta)} = (2-p)t_0^{(p;\beta)} + pt_1^{(p;\beta)}$ takes the same form as for the triplet state (but not the same value, as the Kohn-Sham orbitals for this ensemble are different) and so do the lowest two Hartree-exchange block eigenvalues [given by Eqs. (21) and (22)]. The singlet state has the block eigenvalue

$$\Lambda_{\mathrm{Hx,ss}} = \int \frac{dxdx'}{2} U(x-x')[\phi_0(x)\phi_1(x') + \phi_1(x)\phi_0(x')]^2 , \quad (30)$$

finally yielding the EEXX energy as

$$\begin{aligned} \mathcal{E}_{\mathrm{EEXX}}^{(p;\beta)} =& \mathcal{T}_s^{(p;\beta)} + (1-p)\Lambda_{\mathrm{Hx,gs}}^{(p;\beta)} + p\Lambda_{\mathrm{Hx,ts}}^{(p;\beta)} \\ &+ p\beta[\Lambda_{\mathrm{Hx,ss}}^{(p;\beta)} - \Lambda_{\mathrm{Hx,ts}}^{(p;\beta)}] + \int n^{(p;\beta)} v dx. \end{aligned} \quad (31)$$

With this reasonably straightforward generalization of the pedagogical triplet case, we can now test the suitability of our approach to singlet excitations. To begin our analysis, we show in Fig. 5 the densities of the exact ground-, triplet-, and singlet-states (solid lines), and their KS counterparts (dashed lines) for the difficult case of $R = 2$ and $\mu_S = 2$. In this case, the

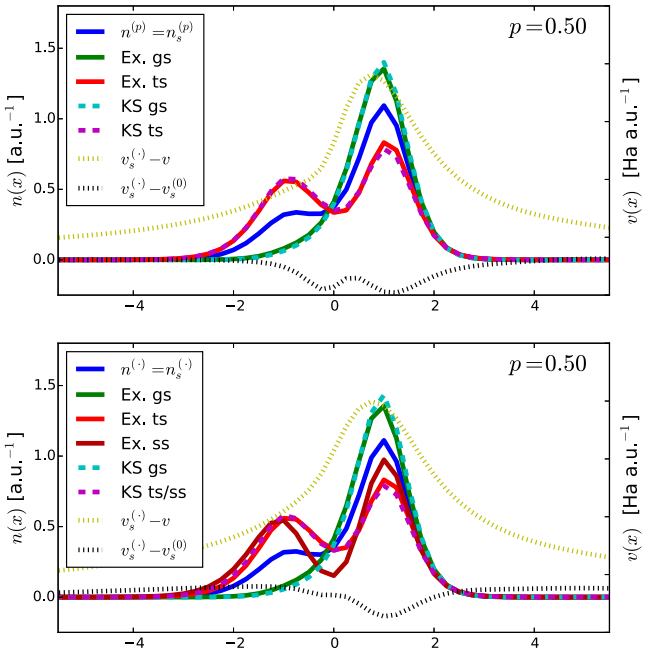

FIG. 5. Exact ($n_{\mathrm{gs/ts(/ss)}}$, solid lines) and Kohn-Sham ($n^{(p)}_{s,\mathrm{gs/ts(/ss)}}$, dashed lines) densities of the ground- and low-lying excited states with $R = 2$ and $\mu_S = 2.0$, calculated from the interacting and non-interacting wavefunctions, respectively, for $p = 0.5$ and $\beta = 0$ (triplet excitation only, top) and $\beta = 0.25$ (singlet excitation included, bottom). Also shown (in dotted lines) are the Hxc potential, $v_{\mathrm{Hxc}}^{(p)/(p,0.25)} = v_s^{(p)/(p,0.25)} - v$, and the ensemble potential difference, $v_s^{(p)/(p,0.25)} - v_s^{(0)}$.

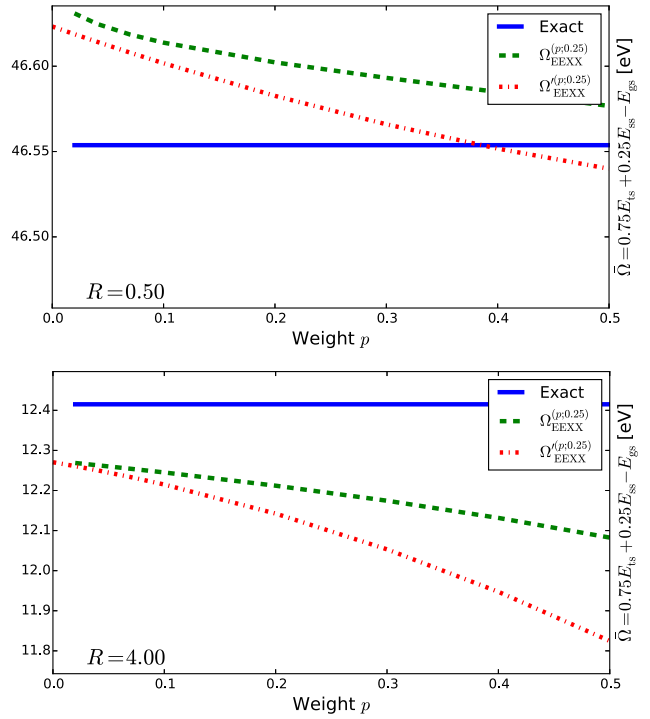

FIG. 6. Exact singlet-triplet averaged energy gap (as obtained in both the many-electron and the exact Kohn-Sham systems), $\bar{\Omega}^{(0.25)}$, compared with that obtained in the two EEXX approximations, $\bar{\Omega}^{(p;0.25)}_{\mathrm{EEXX}}$ and $\bar{\Omega}'^{(p;0.25)}_{\mathrm{EEXX}}$, with $R = 0.5$ (top) and $R = 4$ (bottom) and $\mu_S = 2.0$, which defines a clear charge transfer excitation.

singlet and triplet states possess qualitatively different densities, which must nevertheless still be accommodated by a single KS potential (for the case of $R = 4$, studied in Fig. 2, the singlet/triplet densities are nearly identical, as expected for a negligible singlet-triplet separation). As before, the ground state density is well reproduced. The triplet-singlet average density is also well reproduced and is dominated by the contribution from the triplet state, which is to be expected given the 75% contribution from the triplet state. The KS potential (dots) shows significant differences with respect to that found in Subsection III A (compare Fig. 2), reflecting the different ensemble densities. Here the KS potential appears to have a small step-like feature on the right atom, although this may be a numerical artifact arising from the density inversion. In any case, the step is still small compared to other features and compared to the steps arising in the KS potential of conventional DFT.

The singlet-triplet averaged gap, defined as

$$\bar{\Omega}^{(\beta)} = (1-\beta)E_{\mathrm{ts}} + \beta E_{\mathrm{ss}} - E_{\mathrm{gs}} \equiv \Omega + \beta\Omega_{\mathrm{ss-ts}}, \tag{32}$$

is shown in Fig. 6 both exactly and in the two EEXX approximations,

$$\bar{\Omega}^{(p;\beta)}_{\mathrm{EEXX}} = \frac{\mathcal{E}^{(p;\beta)}_{\mathrm{EEXX}} - \mathcal{E}^{(0;\beta)}_{\mathrm{EEXX}}}{p}, \quad \bar{\Omega}'^{(p;\beta)}_{\mathrm{EEXX}} = \frac{\partial\mathcal{E}^{(p;\beta)}_{\mathrm{EEXX}}}{\partial p}, \tag{33}$$

for $0 \le p \le 0.5$. Here Ω is the optical gap from Eq. (23) and $\Omega_{\mathrm{ss-ts}} = E_{\mathrm{ss}} - E_{\mathrm{ts}}$ is the singlet-triplet splitting energy. For $R = 4$ and $\mu_S = 2$ (bottom), the results are almost identical to the ones given above, reflecting the fact that the singlet-triplet splitting is very small. But for $R = 0.5$ and $\mu_S = 2$ (top), the results are quite different, with the EEXX approximation overestimating the singlet-triplet splitting and thus compensating for some of the missing correlations that led to under-prediction of the excitation energy in the pure triplet example.

Finally, Fig. 7 reproduces the energy curves for the ground- and triplet-states already shown in Fig. 4, but includes also the first excited singlet state energy curve $\Delta E_{\mathrm{ss}}(R) = \Delta E_{\mathrm{ts}}(R) + \Omega_{\mathrm{ss-ts}}(R)$ calculated exactly and at the EEXX level using

$$\Delta E_{\mathrm{EEXX,ss}}(R) = \Delta E_{\mathrm{EEXX,ts}}(R) + \Omega_{\mathrm{EEXX,ss-ts}}(R), \tag{34}$$

where $\Omega_{\mathrm{EEXX,ss-ts}}(R) = 4[\bar{\Omega}^{(0.5,0.25)}_{\mathrm{EEXX}} - \Omega^{(0.5)}_{\mathrm{EEXX}}]$ is the EEXX singlet-triplet splitting energy calculated at $p = 0.5$ and $\beta = 0.25$.

The excited singlet energy dissociation curve obtained with EEXX is not as accurate as in the cases of the ground- and triplet states. This is not surprising, as its energy is likely to have a greater contribution from dynamical correlations which are unaccounted for in EEXX. Nevertheless, the EEXX curve shows good semi-quantitative agreement with the true curve, suggesting that one may devise correlation approximations that can compensate for much of the error. Dissociation curves for cases with stronger correlation (such as $\mu_S = 0$, 1.2, not shown) are, as expected from the poor singlet ground state in these cases, worse.

Finally, we show in Fig. 8 the same ground-, singlet-, and triplet-state energies calculated using time-dependent exact exchange (TDEXX) theory,[17–23] based on the exact ground-state. The TDEXX results are broadly similar in quality to the results from EDFT: triplet excitations are slightly

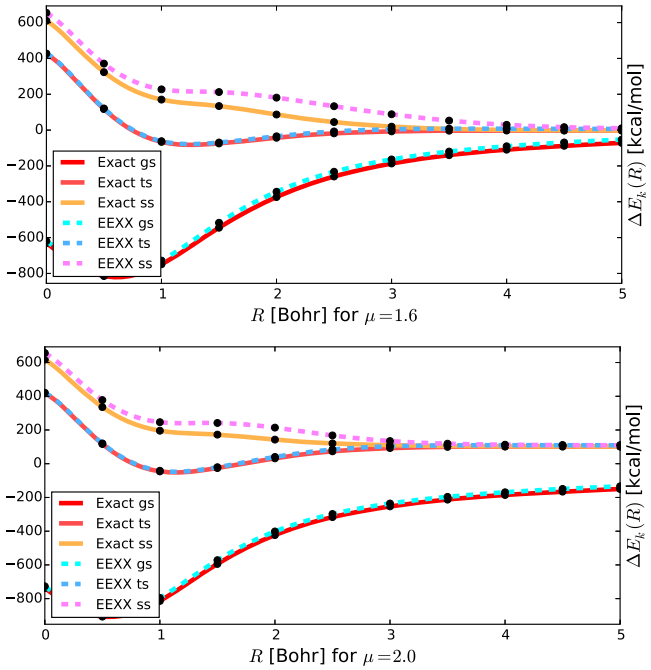

FIG. 7. Exact and Hartree-exchange energy dissociation curves for the ground state, singlet state, and triplet state for $\mu_S = 1.6$ (top) and 2.0 (bottom). EEXX energies are obtained using Eq. (34). The agreement between exact and approximate singlet results is not as good as in the ground- and triplet states, but still has good semi-quantitative behavior.

poorer and singlet excitations are slightly better. This suggests that the most important role is played by the exact exchange contribution employed in both EEXX and TDEXX calculations here, not the time-dependence of the latter. In the two-electron case considered here, TDEXX is straightforward to calculate (details are provided in Appendix C), albeit slightly more difficult than the EEXX calculations reported here.

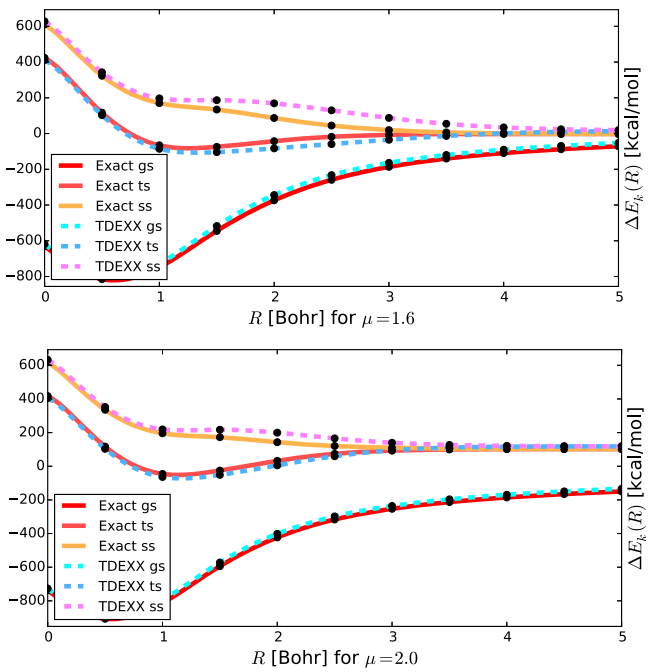

FIG. 8. Exact and time-dependent EXX energy dissociation curves for the ground state, singlet, and triplet state for $\mu_S = 1.6$ (top) and 2.0 (bottom).

However, it has much poorer scaling in general, even in efficient implementations.[19]

IV. CONCLUSION

In this article, we have shown that exact ensemble density functional theory (EDFT), obtained through numerical inversion, can capture charge transfer excitations without relying on time-dependent calculations. In all cases, Kohn-Sham components of the ensemble density were shown to possess a direct physical meaning, despite not being constrained to achieve that.

Approximate excitation energies were obtained at the level of a rigorously extended Hartree-exchange approximation.[33] Results for the triplet state were shown to be good across an entire dissociation curve even when the ground state is bad. For excited singlet state energies, quantitative agreement was not as good as for the ground- and triplet-states, likely owing to dynamic correlation effects. Still, the transitions were well predicted as long as strong correlations were not present. Results were shown to be comparable in quality to more numerically intensive TDEXX calculations, suggesting that EDFT may give similar accuracy to TDDFT at the same level of approximation, but at lower cost.

Importantly, the effective Kohn-Sham potential needed to produce these results was found to lack a difficult-to-approximate complex step structure that can appear in other formalisms, at least when only triplets were considered. A small step may be present in the difficult-to-reproduce case of an excited singlet state with a density highly unlike that of the corresponding triplet state; even then it is significantly smaller in magnitude than other features of the potential. This may indicate that the effective potential for ensembles is more amenable to useful approximations for the difficult case of molecular dissociation than the potentials in other density-based formulations.

Strictly speaking, the calculations presented here apply to simplified one-dimensional model systems. In particular, the role played by differences between the densities and their non-interacting KS counterparts warrants further consideration. Nevertheless, we believe that these results are sufficiently fundamental to be replicated in more realistic molecules, a case further supported by recent approximate EDFT work.[35] This work provides robust previously unavailable benchmarks and provides impetus for establishing EDFT correlation functionals that will allow systematic improvements.

ACKNOWLEDGMENTS

L.K. acknowledges support by the Israel Science Foundation.

APPENDIX A: THE Λ_{Hx} FUNCTIONALS

We summarize here the key features of Λ_{Hx} in the case of the ground- and lowest lying excited state of "typical"

systems without spatial degeneracies. The key to deriving these expressions is to recognize that $\Lambda_{\rm Hx}[n;\mathcal{W}]$ are eigenvalues of block sub-matrices of $\langle\Psi_\kappa|\hat{W}|\Psi_{\kappa'}\rangle$, taken over states with identical densities and kinetic energies, and ordered from smallest to largest within each block. Full details, and derivation, of the minimization procedure used to derive the resulting "block eigenvalues" can be found in the main article and the supplementary material of Ref. 33.

In the case considered here, the KS ground state with ϕ_0 doubly occupied is non-degenerate, and therefore no other state shares its density $n_{s,\rm gs} = 2|\phi_0|^2$ or kinetic energy $T_{s,\rm gs} = 2t_0$. The first excited state is *four-fold* degenerate at the density/kinetic energy level, however, as the states ϕ_0 and ϕ_1 can take on any combination of $\uparrow$ and $\downarrow$ spins in our spin-unpolarized formalism, while preserving $n_{s,\rm ts} = n_{s,\rm ss} = |\phi_0|^2 + |\phi_1|^2$ and $T_{s,\rm ts} = T_{s,\rm ss} = t_0 + t_1$. Note that here these states are all degenerate—the triplet/singlet splitting is distinguished only in the next step.

Because it is non-degenerate, we can calculate $\Lambda_{\rm Hx,gs} = \langle 0\uparrow, 0\downarrow|\hat{W}|0\uparrow, 0\downarrow\rangle$ directly for use in $\mathcal{E}_{\rm Hx}$. But once triplet and singlet states are involved, we must find the eigenvalues of

$$\mathbb{W} = \begin{pmatrix} \langle\uparrow\uparrow|\hat{W}|\uparrow\uparrow\rangle & \langle\uparrow\uparrow|\hat{W}|\uparrow\downarrow\rangle & \langle\uparrow\uparrow|\hat{W}|\downarrow\uparrow\rangle & \langle\uparrow\uparrow|\hat{W}|\downarrow\downarrow\rangle \\ \langle\uparrow\downarrow|\hat{W}|\uparrow\uparrow\rangle & \langle\uparrow\downarrow|\hat{W}|\uparrow\downarrow\rangle & \langle\uparrow\downarrow|\hat{W}|\downarrow\uparrow\rangle & \langle\uparrow\downarrow|\hat{W}|\downarrow\downarrow\rangle \\ \langle\downarrow\uparrow|\hat{W}|\uparrow\uparrow\rangle & \langle\downarrow\uparrow|\hat{W}|\uparrow\downarrow\rangle & \langle\downarrow\uparrow|\hat{W}|\downarrow\uparrow\rangle & \langle\downarrow\uparrow|\hat{W}|\downarrow\downarrow\rangle \\ \langle\downarrow\downarrow|\hat{W}|\uparrow\uparrow\rangle & \langle\downarrow\downarrow|\hat{W}|\uparrow\downarrow\rangle & \langle\downarrow\downarrow|\hat{W}|\downarrow\uparrow\rangle & \langle\downarrow\downarrow|\hat{W}|\downarrow\downarrow\rangle \end{pmatrix},$$

where $|\sigma\sigma'\rangle$ is short-hand for $|0\sigma, 1\sigma'\rangle$, to determine $\mathcal{E}_{\rm Hx}$. One can use the Slater-Condon rules to eliminate many of the terms in $\mathbb{W}$, from which one finds the three-fold degenerate lowest eigenvalue $\Lambda_{\rm Hx,ts} = \langle 0\uparrow, 1\uparrow|\hat{W}|0\uparrow, 1\uparrow\rangle = \langle 0\downarrow, 1\downarrow|\hat{W}|0\downarrow, 1\downarrow\rangle = \langle 0\uparrow, 1\downarrow|\hat{W}|0\uparrow, 1\downarrow\rangle + \langle 0\uparrow, 1\downarrow|\hat{W}|0\downarrow, 1\uparrow\rangle$ and the higher energy singlet state $\Lambda_{\rm Hx,ss} = \langle 0\uparrow, 1\downarrow|\hat{W}|0\uparrow, 1\downarrow\rangle - \langle 0\uparrow, 1\downarrow|\hat{W}|0\downarrow, 1\uparrow\rangle$. Both inherit the correct spin qualities via the diagonalization of $\mathbb{W}$.

Finally, we can expand these out to find

$$\Lambda_{\rm Hx,gs} = \int \frac{dxdx'}{2} U(x-x') 2\phi_0(x)^2\phi_0(x')^2,$$

$$\Lambda_{\rm Hx,ts} = \int \frac{dxdx'}{2} U(x-x')[\phi_0(x)\phi_1(x') - \phi_1(x)\phi_0(x')]^2,$$

$$\Lambda_{\rm Hx,ss} = \int \frac{dxdx'}{2} U(x-x')[\phi_0(x)\phi_1(x') + \phi_1(x)\phi_0(x')]^2$$

in our specific case, as in Eqs. (21), (22), and (30). The Hx energy is then given by

$$\mathcal{E}_{\rm Hx} = w_{\rm gs}\Lambda_{\rm Hx,gs} + w_{\rm ts}\Lambda_{\rm Hx,ts} + w_{\rm ss}\Lambda_{\rm Hx,ss}. \tag{A1}$$

APPENDIX B: THE DIFFERENCE BETWEEN EXACT AND KS DENSITIES

Equation (17), restated here for convenience,

$$\begin{aligned} n^{(p)} &= (1-p)n_{\rm gs} + pn_{\rm ts} = (1-p)n^{(p)}_{s,\rm gs} + pn^{(p)}_{t,\rm ts} \\ &= (2-p)|\phi_0^{(p)}|^2 + p|\phi_1^{(p)}|^2, \end{aligned} \tag{B1}$$

shows the relationship between the exact and Kohn-Sham densities, and the two orbitals that go into the latter. It may be tempting, at first glance, to assume that $n_{\rm gs} = n^{(p)}_{s,\rm gs}$ and $n_{\rm ts} = n^{(p)}_{s,\rm ts}$. As illustrated below, this is not the case in general, and any similarity between the real and KS densities, i.e., $n_{\rm gs} \approx n^{(p)}_{s,\rm gs}$ and $n_{\rm ts} \approx n^{(p)}_{s,\rm ts}$, highlights a success of the EDFT formalism in retaining an intuitive understanding of the densities involved.

The latter point is most obvious when we consider a singlet state as well. We note that the triplet- and singlet-densities of interacting states are not the same, i.e., $n_{ts} \neq n_{\rm ss}$ in general (see, e.g., Fig. 5). However, as noted in Sec. III B, the corresponding KS densities are independent of the choice of spins, and $n_{s,\rm ts} = n_{s,ss} = |\phi_0|^2 + |\phi_1|^2$ are identical. Ergo, the KS densities cannot be the same as the interacting densities. In the singlet/triplet case, having $n_{s,\rm gs} = |\phi_0|^2 = n_{\rm gs}$ would require, at a minimum, that $n_{\rm ts} - n_{\rm gs}/2 = n_{s,\rm ts} - n_{s,\rm gs} = |\phi_1|^2 > 0$, a situation that cannot be guaranteed in general.

Another perspective to this issue is provided by considering the degrees of freedom available to the problem. Both ϕ_0 and ϕ_1 must, by virtue of the GOK generalization of the Hohenberg-Kohn theorem, be eigenfunctions of the same one-body Hamiltonian $\hat{h}_s = \hat{t} + \hat{v}_s$, where the multiplicative potential v_s acts as a continuous Lagrange multiplier that constrains the non-interacting density n_s to be equal to n. Thus $n_{s,\rm gs} = 2|\phi_0|^2$ and $n_{s,\rm ts} = |\phi_0|^2 + |\phi_1|^2$ come from a constrained problem with just one continuous Lagrange multiplier, v_s, for one continuous constraint, $(2-p)|\phi_0^2| + p|\phi_1^2| = n^{(p)}$. Matching the components of the density $n_{\rm gs}$ and $n_{\rm ts}$ separately would require *two* continuous constraints. But in this case we have *three densities*, $n_{\rm gs}$, $n_{\rm ts}$, and $n_{\rm ss}$, that must be reproduced by just *two orbitals* coming from a *single potential* v_s—clearly an impossible task in general. Quite generally, any new density would require its own Lagrange multiplier. Hence, given the over-constrained nature of the problem, it is fortunate and not at all obvious that the KS densities $n_{s,\kappa}$ of components even qualitatively resemble their interacting counterparts n_κ.

APPENDIX C: TIME-DEPENDENT EXACT EXCHANGE CALCULATIONS

The time-dependent exact exchange results presented here are calculated using linear response theory as follows. First, we write the spin-resolved response function as

$$\chi_{0,\sigma\sigma'}(x,x') = -\delta_{\sigma\sigma'}\sum_a C_{0a}(\omega)\rho_{0a}(x)\rho_{0a}(x'), \tag{C1}$$

using the transition densities $\rho_{0a}(x) = \phi_0(x)\phi_a(x)$, with $a > 0$ designating an unoccupied orbital. Here, $C_{0a} = \frac{\epsilon_a - \epsilon_0}{(\epsilon_a-\epsilon_0)^2+\omega^2}$. We can then expand the interacting response in the same basis, to obtain

$$\chi_{\sigma\sigma'}(x,x') = -\sum_{aa'} C_{aa'\sigma\sigma'}(\omega)\rho_{0a}(x)\rho_{0a}(x'), \tag{C2}$$

where $C_{aa'\sigma\sigma'} = C_{0,a}\delta_{aa'\sigma\sigma'} - C_{0,a\sigma}f_{{\rm Hx},aa''\sigma\sigma''}C_{a''a'\sigma''\sigma'}$ and $f_{{\rm Hx},aa'\sigma\sigma'} = \int dxdx' f_{{\rm Hx},\sigma\sigma'}(x,x')\rho_{0a}(x)\rho_{0a'}(x')$ is the Hartree-exchange kernel projected onto the basis of the transition densities. In the exact exchange approximation for the two-electron case, only the electrons of opposite spin can interact, to avoid spurious self-interactions. Thus, $f_{{\rm Hx},\sigma\sigma'} = 0$ for $\sigma = \sigma'$ and $f_{{\rm Hx},\sigma\sigma'}(x,x') = U(x,x')$ for $\sigma \neq \sigma'$.

To obtain the transition energies, we seek the frequencies ω for which the denominator of $\chi_{\sigma\sigma'}$ is zero. After some algebra along the lines of the derivation of the Casida equation,[74] it can be shown that these occur for the eigenvalues $\Omega_a^{\mathrm{TDEXX}}$ of the matrix

$$\mathbb{T} \equiv \mathrm{diag}[\epsilon_a - \epsilon_0]\delta_{\sigma\sigma'} + (1 - \delta_{\sigma\sigma'})U_{0a,0a'}, \tag{C3}$$

where $U_{0a,0a'} = \int dxdx' U(x,x')\rho_{0a}(x)\rho_{0a'}(x')$. Then, we diagonalize $\mathbb{T}$ using 50 excited state orbitals, resulting in a 100×100 matrix after accounting for spin. This has been found to be more than sufficient to converge the transition energies to the complete basis set limit. Finally, we add the lowest two transition frequencies thus obtained ($\Omega_1^{\mathrm{TDEXX}}$ and $\Omega_2^{\mathrm{TDEXX}}$) to the ground-state EXX energy of the system, to obtain the energies of the singlet and triplet states, respectively.

[1] P. Hohenberg and W. Kohn, Phys. Rev. **136**, B864 (1964).
[2] W. Kohn and L. J. Sham, Phys. Rev. **140**, A1133 (1965).
[3] E. Runge and E. K. U. Gross, Phys. Rev. Lett. **52**, 997 (1984).
[4] C. S. De Castro, S. Dimitrov, H. D. Burros, P. Douglas, and M. L. Davies, Sci. Prog. **100**, 212 (2017).
[5] S. Kumar, K. Ojha, and A. K. Ganguli, Adv. Mater. Interfaces **4**, 1600981 (2017).
[6] G. J. Hedley, A. Ruseckas, and I. Samuel, Chem. Rev. **117**, 796 (2017).
[7] N. T. Maitra, J. Phys.: Condens. Matter **29**, 423001 (2017).
[8] S. Kümmel, Adv. Energy Mater. **7**, 1700440 (2017).
[9] M. Thiele and S. Kümmel, Phys. Rev. Lett. **112**, 083001 (2014).
[10] D. J. Tozer, R. D. Amos, N. C. Handy, B. O. Roos, and L. Serrano-Andres, Mol. Phys. **97**, 859 (1999).
[11] B. Kaduk, T. Kowalczyk, and T. Van Voorhis, Chem. Rev. **112**, 321 (2012).
[12] L. Kronik, T. Stein, S. Refaely-Abramson, and R. Baer, J. Chem. Theory Comput. **8**, 1515 (2012).
[13] A. Seidl, A. Görling, P. Vogl, J. A. Majewski, and M. Levy, Phys. Rev. B **53**, 3764 (1996).
[14] T. Stein, L. Kronik, and R. Baer, J. Am. Chem. Soc. **131**, 2818 (2009).
[15] T. Stein, L. Kronik, and R. Baer, J. Chem. Phys. **131**, 244119 (2009).
[16] A. Karolewski, L. Kronik, and S. Kümmel, J. Chem. Phys. **138**, 204115 (2013).
[17] A. Görling, Int. J. Quantum Chem. **69**, 265 (1998).
[18] M. Hellgren and U. von Barth, Phys. Rev. B **78**, 115107 (2008).
[19] A. Hesselmann and A. Görling, Mol. Phys. **108**, 359 (2010).
[20] M. Hellgren and U. von Barth, J. Chem. Phys. **132**, 044101 (2010).
[21] M. Hellgren and E. K. U. Gross, Phys. Rev. A **85**, 022514 (2012).
[22] P. Bleiziffer, A. Hesselmann, and A. Görling, J. Chem. Phys. **136**, 134102 (2012).
[23] M. Hellgren and E. K. U. Gross, Phys. Rev. A **88**, 052507 (2013).
[24] E. K. U. Gross, L. N. Oliveira, and W. Kohn, Phys. Rev. A **37**, 2805 (1988).
[25] E. K. U. Gross, L. N. Oliveira, and W. Kohn, Phys. Rev. A **37**, 2809 (1988).
[26] L. N. Oliveira, E. K. U. Gross, and W. Kohn, Phys. Rev. A **37**, 2821 (1988).
[27] A. K. Theophilou, J. Phys. C: Solid State Phys. **12**, 5419 (1979).
[28] S. M. Valone, J. Chem. Phys. **73**, 4653 (1980).
[29] J. P. Perdew, R. G. Parr, M. Levy, and J. L. Balduz, Phys. Rev. Lett. **49**, 1691 (1982).
[30] E. H. Lieb, Int. J. Quantum Chem. **24**, 243 (1983).
[31] A. Savin, *On Degeneracy, Near-Degeneracy and Density Functional Theory* (Elsevier, Amsterdam, 1996), pp. 327–358.
[32] P. W. Ayers, Phys. Rev. A **73**, 012513 (2006).
[33] T. Gould and S. Pittalis, Phys. Rev. Lett. **119**, 243001 (2017).
[34] O. Franck and E. Fromager, Mol. Phys. **112**, 1684 (2014).
[35] M. Filatov, M. Huix-Rotllant, and I. Burghardt, J. Chem. Phys. **142**, 184104 (2015).
[36] M. Filatov, "Ensemble DFT approach to excited states of strongly correlated molecular systems," in *Density-Functional Methods for Excited States*, edited by N. Ferré, M. Filatov, and M. Huix-Rotllant (Springer International Publishing, Cham, 2016), pp. 97–124.
[37] K. Deur, L. Mazouin, and E. Fromager, Phys. Rev. B **95**, 035120 (2017).
[38] Z.-h. Yang, J. R. Trail, A. Pribram-Jones, K. Burke, R. J. Needs, and C. A. Ullrich, Phys. Rev. A **90**, 042501 (2014).
[39] A. Pribram-Jones, Z.-h. Yang, J. R. Trail, K. Burke, R. J. Needs, and C. A. Ullrich, J. Chem. Phys. **140**, 18A541 (2014).
[40] Z.-h. Yang, A. Pribram-Jones, K. Burke, and C. A. Ullrich, Phys. Rev. Lett. **119**, 033003 (2017).
[41] W. Yang, Y. Zhang, and P. W. Ayers, Phys. Rev. Lett. **84**, 5172 (2000).
[42] Á. Nagy, S. Liu, and L. Bartolloti, J. Chem. Phys. **122**, 134107 (2005).
[43] S. Pittalis, S. Kurth, and E. Gross, J. Chem. Phys. **125**, 084105 (2006).
[44] T. Gould and J. F. Dobson, J. Chem. Phys. **138**, 014103 (2013).
[45] E. Kraisler and L. Kronik, Phys. Rev. Lett. **110**, 126403 (2013).
[46] E. Kraisler and L. Kronik, J. Chem. Phys. **140**, 18A540 (2014).
[47] A. Görling, Phys. Rev. B **91**, 245120 (2015).
[48] P. Elliott, K. Burke, M. H. Cohen, and A. Wasserman, Phys. Rev. A **82**, 024501 (2010).
[49] R. Tang, J. Nafziger, and A. Wasserman, Phys. Chem. Chem. Phys. **14**, 7780 (2012).
[50] M. S. Gordon, D. G. Fedorov, S. R. Pruitt, and L. V. Slipchenko, Chem. Rev. **112**, 632 (2012).
[51] E. Fabiano, S. Laricchia, and F. Della Sala, J. Chem. Phys. **140**, 114101 (2014).
[52] J. Nafziger and A. Wasserman, J. Chem. Phys. **143**, 234105 (2015).
[53] N. I. Gidopoulos, P. G. Papaconstantinou, and E. K. U. Gross, Phys. Rev. Lett. **88**, 033003 (2002).
[54] M. Levy, Proc. Natl. Acad. Sci. U. S. A. **76**, 6062 (1979).
[55] J. Harris, Phys. Rev. A **29**, 1648 (1984).
[56] J. P. Perdew and K. Schmidt, in *Density Functional Theory and Its Application to Materials*, edited by V. Van Doren, C. Van Alsenoy, and P. Geerlings (American Institute of Physics, New York, 2001), pp. 1–20.
[57] S. Kümmel and L. Kronik, Rev. Mod. Phys. **80**, 3 (2008).
[58] K. Burke, J. Chem. Phys. **136**, 150901 (2012).
[59] A. D. Becke, J. Chem. Phys. **140**, 18A301 (2014).
[60] R. O. Jones, Rev. Mod. Phys. **87**, 897 (2015).
[61] M. Levy, Phys. Rev. A **26**, 1200 (1982).
[62] C. Li and W. Yang, J. Chem. Phys. **146**, 074107 (2017).
[63] R. T. Sharp and G. K. Horton, Phys. Rev. **90**, 317 (1953).
[64] J. D. Talman and W. F. Shadwick, Phys. Rev. A **14**, 36 (1976).
[65] M.-C. Kim, E. Sim, and K. Burke, Phys. Rev. Lett. **111**, 073003 (2013).
[66] For our calculations, we employ a grid with $x \in [-9, 9]$ distributed at intervals of $\Delta x = 0.25$. Derivatives are calculated using 7-point formulae and assuming $f(|x| > 9) = 0$. The greatest errors in our implementation come from quadratures, which are everywhere defined as $\int f(x)dx \approx \sum_i f(x_i)\Delta x$. Through this choice, we avoid inconsistencies at different stages of the calculations, at the expense of absolute accuracy. Density inversions are captured using a heuristic variant of the approach of Ref. 67. Code is available on request.
[67] T. Gould and J. Toulouse, Phys. Rev. A **90**, 050502 (2014).
[68] G. M. J. Barca, A. T. B. Gilbert, and P. M. W. Gill, J. Chem. Phys. **141**, 111104 (2014).
[69] A. Karolewski, R. Armiento, and S. Kümmel, J. Chem. Theory Comput. **5**, 712 (2009).
[70] E. Kraisler and L. Kronik, Phys. Rev. A **91**, 032504 (2015).
[71] P. Gori-Giorgi and A. Savin, J. Phys.: Conf. Ser. **117**, 012017 (2008).
[72] B. I. Dunlap, "Symmetry and degeneracy in Xα and density functional theory," in *Advances in Chemical Physics* (John Wiley & Sons, Inc., 1983), pp. 287–318.
[73] M. J. Peach, M. J. Williamson, and D. J. Tozer, J. Chem. Theory Comput. **7**, 3578 (2011).
[74] M. E. Casida, "Time-dependent density functional response theory for molecules," in *Recent Advances in Density Functional Methods*, edited by D. P. Chong (World Scientific, Singapore, 1995), pp. 155–192.